

# $p$ -DkNN: Out-of-Distribution Detection Through Statistical Testing of Deep Representations

Adam Dziedzic\*  
University of Toronto & Vector Institute  
adam.dziedzic@utoronto.ca

Stephan Rabanser\*  
University of Toronto & Vector Institute  
stephan@cs.toronto.edu

Mohammad Yaghini\*  
University of Toronto & Vector Institute  
mohammad.yaghini@mail.utoronto.ca

Armin Ale  
University of Toronto & Vector Institute  
seyedarmin.alemohammad@mail.utoronto.ca

Murat A. Erdogdu  
University of Toronto & Vector Institute  
erdogdu@cs.toronto.edu

Nicolas Papernot  
University of Toronto & Vector Institute  
nicolas.papernot@utoronto.ca

## Abstract

The lack of well-calibrated confidence estimates makes neural networks inadequate in safety-critical domains such as autonomous driving or healthcare. In these settings, having the ability to abstain from making a prediction on out-of-distribution (OOD) data can be as important as correctly classifying in-distribution data. We introduce  $p$ -DkNN, a novel inference procedure that takes a trained deep neural network and analyzes the similarity structures of its intermediate hidden representations to compute  $p$ -values associated with the end-to-end model prediction. The intuition is that statistical tests performed on latent representations can serve not only as a classifier, but also offer a statistically well-founded estimation of uncertainty.  $p$ -DkNN is scalable and leverages the composition of representations learned by hidden layers, which makes deep representation learning successful. Our theoretical analysis builds on Neyman-Pearson classification and connects it to recent advances in selective classification (*reject option*). We demonstrate advantageous trade-offs between abstaining from predicting on OOD inputs and maintaining high accuracy on in-distribution inputs. We find that  $p$ -DkNN forces adaptive attackers crafting adversarial examples, a form of worst-case OOD inputs, to introduce semantically meaningful changes to the inputs.

## 1 Introduction

While deep representation learning can generalize well to in-distribution test data, the ability of neural networks to generalize—or even detect—out-of-distribution data remains weak (Nagarajan et al., 2021). This is an obstacle to their deployment in tasks which raise concerns of safety (e.g., autonomous driving (Jain et al., 2019; Ghodsi et al., 2021; Wang et al., 2021)), security (e.g., malware detection (Anderson et al.,

---

\*Equal contribution.

2017)), or ethics (e.g., fairness of lending decisions (Liu et al., 2018; Chen, 2018)). Certain approaches to machine learning promise to address this limitation by inherently modeling uncertainty. This is best exemplified by Bayesian neural networks, which model the distribution of each weight in the neural network to naturally obtain a distribution of outputs from which uncertainty can be estimated. Unfortunately, this class of approaches often lacks scalability (Gal et al., 2014; Gustafsson et al., 2020).

In this paper, we instead reason about uncertainty in the paradigm of frequentist statistics. The crux of our approach relies on the observation that a statistical test can be a natural classifier. Furthermore, this classifier comes with the added benefit of modeling type I error, i.e., the ability to abstain from making a prediction when significance is too low. It is thus a compelling option to both model uncertainty and detection of out-of-distribution samples fed into the classifier.

To combine the advantages of this frequentist approach with those of deep representation learning, we propose to leave the training algorithm for deep neural networks (DNNs) intact but modify how one uses a trained model for inference. Our prediction procedure exploits the modularity of DNNs: each hidden layer outputs a different learned representation whose similarity structure helps us characterize the data distribution of interest. We analyze these similarity structures to compute a  $p$ -value associated with accepting each possible label. Our analysis shares some intuition with the Deep k-Nearest Neighbor (Papernot and McDaniel, 2018), hereafter abbreviated as DkNN, where a nearest neighbor search in representation spaces learned by each of the hidden layers serves as the basis for predicting on a test input—in lieu of directly outputting the result of a forward pass through the neural network. While Papernot and McDaniel (2018) reported promising initial results for out-of-distribution detection, including adversarial examples (Biggio et al., 2013; Szegedy et al., 2014), DkNN’s uncertainty estimation is not statistically well-founded.

To remediate these pitfalls, we propose a novel inference procedure called  $p$ -DkNN, which computes proper  $p$ -values. At inference time,  $p$ -values are calculated through pairwise testing of mean distances between the test input and  $k$ -closest neighbors in each class and layer. Similar approaches also based on statistical hypothesis testing of nearest neighbor latent representations have recently been proposed by Raghuram et al. (2020). While strongly related, their work introduces new test statistic based on log-likelihood-ratios between nearest-neighbor class counts. Furthermore, they make the assumption that tests across layers are independent to aggregate them. Our approach on the other hand uses proven off-the-shelf testing statistics and employs aggregation methods that do not impose any independence assumptions. We combine  $p$ -values using known statistical techniques to obtain a meaningful single metric of uncertainty for the entire model.

Our statistical testing evaluates the probability of each class regardless of whether this is the correct class or not, whereas prior approaches evaluated the probability of a given class assuming that it was the correct class.

$p$ -DkNN is a skeptical/cautious method by design. Abstaining is the default action since that is our null hypothesis throughout the tests.

This has advantages which are not without raising new difficulties when it comes with defining and evaluating what constitute good performance from the classifier. In the majority of the ML literature the focus is on minimizing the risk, which is a weighted sum of false positive and false negative

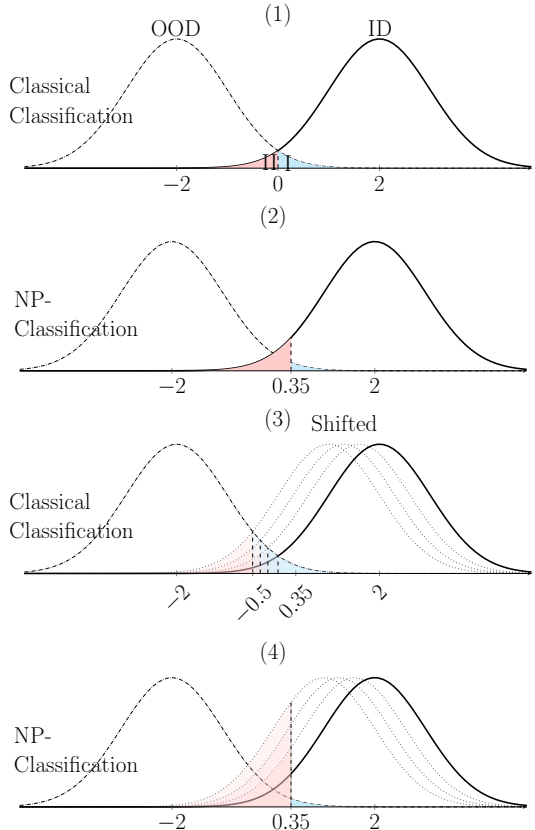


Figure 1: Selection of in-distribution samples using classical (1) vs. NP (2) classification where the Type I error  $< 0.05$ . (3) and (4) repeat this in the presence of distribution shifts. An NP-classifier gives a Type I error guarantee at the expense of higher Type II error.

rates. Instead, robust classification is a multi-objective optimization problem. Robust classifiers require us to step away from the assumption that sample distributions are the same (or even close) at train and inference time. As a result, a robust classifier has two (possibly competing) objectives: **(i)** selecting the correct samples to classify (the selection step, or *S-step*), and **(ii)** classifying the selected samples accurately (classification step, or *C-step*). Consequently, the performance metrics are also different for each goal: for the latter, we want to have the best accuracy, whereas for the former, it is more important for a robust classifier to abstain from selecting incorrect samples (small Type I error / low false positive rate) than to erroneously discard some correct ones: e.g., classifying a malicious tumor as benign is a deadly mistake compared to misclassifying a benign tumor as malicious.

The Neyman-Pearson (NP-) classification is a more appropriate framework than empirical risk minimization since it bounds the most dangerous error (typically called Type I error) at the expense of the less significant error (Type II). We posit that for safety or security critical classifiers that may be provided arbitrary samples at inference time, a selection step should precede the actual classification; and that NP-classification is an appropriate framework for that.

Our empirical evaluation of  $p$ -DkNN in Section 5 commences with the calibration of our predictor. This includes tuning the number of nearest neighbors and search for other hyperparameters to optimally compute and aggregate  $p$ -values, for example, we adjust the significance level. Then, we evaluate the  $p$ -DkNN on standard vision datasets (MNIST, FashionMNIST, SVHN, GTSRB, and CIFAR10) to show that (1) it is able to reject out-of-distribution inputs while continuing to correctly classify in-distribution inputs; (2) it offers better trade-offs between accuracy and false positives on legitimate data than prior approaches including DkNN or Trust (Jiang et al., 2018); and (3) it also offers some robustness to attackers crafting worst-case out-of-distribution inputs such as (adaptive) adversarial examples. We note that for (1) and (2) we focus on a safety scenario where out-of-distribution data is *natural* (e.g., from a different dataset of the same modality) whereas in (3) we switch to a security-motivated setting where out-of-distribution examples are *crafted* by an adversary. Thus, security implies safety, but the converse is not true.

To summarize, our contributions are as follows:

- We introduce the  $p$ -DkNN inference procedure which takes in a trained DNN and incorporates validation data at test time to output  $p$ -values and effect sizes capturing prediction uncertainty.
- We theoretically analyze properties of  $p$ -DkNN to establish a connection to recent advances in selective classification. In particular, we show that  $p$ -DkNN is a PQ-Learner (Goldwasser et al., 2020).
- We empirically demonstrate that  $p$ -DkNN abstains from predicting on out-of-distribution inputs while maintaining high accuracy on in-distribution inputs. In the presence of an adversary aware of  $p$ -DkNN, we show that adversarial examples able to evade  $p$ -DkNN are more likely to introduce semantically meaningful changes to the input—thus defeating the purpose of the attack.

## 2 Related Work

**Uncertainty Quantification in Deep Learning.** High-stakes decision-making domains call for proper uncertainty estimates along with point prediction such that risk can be effectively minimized (Gal, 2016). From a Bayesian viewpoint, Gaussian processes (Rasmussen, 2003) offer a principled way of quantifying uncertainty by modeling the probability distribution over all possible functions that fit the data. Although mathematically elegant, Gaussian processes usually fail at scaling to complex data modeling tasks. As an alternative to Gaussian processes, Bayesian neural networks offer a natural way of accounting for full predictive uncertainty by estimating a probability distribution over the model’s parameters. In order to be practically feasible, techniques from variational inference (Blundell et al., 2015) or Markov chain Monte Carlo (MCMC) (Koller and Friedman, 2009) are used to compute an approximate posterior over the model’s parameters. To further reduce the computational cost, Monte Carlo dropout (Gal and Ghahramani, 2016) can be applied to yield predictive uncertainty measures by performing dropout at test time. When taking a frequentist viewpoint, ensembling techniques (Lakshminarayanan et al., 2016) combine multiple models that are either trained on different subsets of the training data or trained using different weight initializations. Finally, our work is perhaps closest to the Deep k-Nearest Neighbors (DkNN) (Papernot and McDaniel, 2018) which we covered in the introduction.

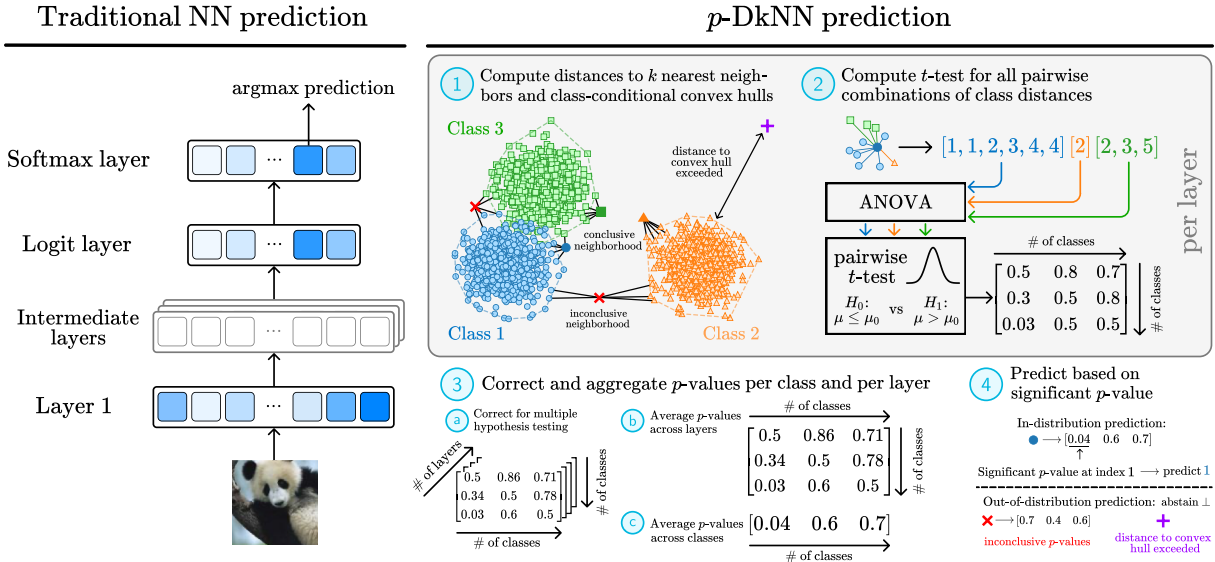


Figure 2: **Overview of  $p$ -DkNN vs traditional DNN classification.** For a given test input, we compute the representations across all latent layers and estimate the nearest neighbor distances with respect to activations of a validation set. After passing an ANOVA test, these distances are fed into a sequence of pairwise  $t$ -tests. The resulting  $p$ -value tensor is then corrected for multiple hypothesis testing and aggregated to a single vector of class- $p$ -values. Significant  $p$ -values yield a class prediction, otherwise we abstain. We also abstain if a data point is too far from a predicted class’ convex hull. Effect sizes are omitted for clarity.

**OOD, Safety, and Security.** In our work, we consider OOD detection in the context of both safety and security. By safety, we mean settings where the model may be presented with naturally occurring OOD inputs (Amodei et al., 2016). This is the case for naturally occurring transformations of the input, which can prove to be challenging even for state-of-the-art vision models (Ford et al., 2019; Hendrycks and Dietterich, 2018). Instead, when we consider an adversary attacking our model, its security will stem from the ability to detect malicious OOD inputs such as adversarial examples (Biggio et al., 2013; Szegedy et al., 2014) or recover the correct labels for them. Many recent lines of works studied different causes of adversarial examples, postulating linearity and over-parametrization as possible culprits (Biggio et al., 2013; Goodfellow et al., 2014). An intuitive explanation is that adversarial examples are caused by small measure regions of adversarial class *jutting* into a correct decision region (Roth et al., 2019). This model is commonly accepted since the clean in-distribution samples remain correctly classified when perturbed with small random noise (e.g., Uniform or Gaussian). Adversarial examples directly exploit the poor generalization of neural networks and this makes them difficult to detect or correct their predictions. We experiment with standard attacks, such as FGSM and PGD, as well as adaptive white-box attacks, for example, the feature adversaries introduced by Sabour et al. (2016).

### 3 Methods

We propose  $p$ -DkNN which takes a DNN trained using an off-the-shelf optimizer and adapts its inference procedure to harness statistical hypothesis testing of intermediate layer representations. Rather than taking the argmax of the softmax output layer,  $p$ -DkNN performs prediction by computing distances between internal representations of a given test point and the representations of all points from a validation set  $\mathbf{X} \in \mathbb{R}^{V \times D}$ , for which label information  $\mathbf{y} \in [C]^V$  is available, across all layers and feeding these distances into a sequence of statistical hypothesis tests and subsequent aggregation methods<sup>1</sup>. We depict  $p$ -DkNN’s

<sup>1</sup>To aid generalization, we fit the underlying neural network classifier using *training* data while  $p$ -DkNN’s inference procedure relies on computing distances to a *validation* set.

prediction stage in Figure 2 and provide an overview in Algorithm 1.

### 3.1 Distance computation

For a given test input  $\tilde{\mathbf{x}} \in \mathbb{R}^D$ ,  $p$ -DkNN starts by computing the activations  $\{\tilde{\mathbf{x}}_\lambda\}_{\lambda=1}^L$  of  $\tilde{\mathbf{x}}$  for all layers  $\lambda$  by performing a forward pass through the network. Then, for each layer  $\lambda$ , we compute the  $\ell_2$  distances between the test point’s representation at layer  $\lambda$ , i.e.  $\tilde{\mathbf{x}}_\lambda$ , and the representations of all data points from a validation set  $\{\mathbf{X}_\lambda\}_{\lambda=1}^L$ . We collect these distances in  $\boldsymbol{\mu} \in \mathbb{R}^V$  with entries  $\boldsymbol{\mu}_j = \|\mathbf{X}_{\lambda,j} - \tilde{\mathbf{x}}_\lambda\|_2$ . To estimate the distances and labels of the validation points in the neighborhood of  $\tilde{\mathbf{x}}$  only, we select the first  $k$  elements of  $\boldsymbol{\mu}$  in ascending order. We store these  $k$ -nearest-neighbor distances and their corresponding ground truth labels in  $\hat{\boldsymbol{\mu}} \in \mathbb{R}^k$  and  $\hat{\mathbf{y}} \in [C]^k$ , respectively.

### 3.2 Classification by means of hypothesis testing

Having obtained  $\hat{\boldsymbol{\mu}}$  and  $\hat{\mathbf{y}}$  at a particular layer  $\lambda$ , we want to determine whether there is sufficient evidence encoded in the distances such that the test point  $\tilde{\mathbf{x}}$  can be confidently assigned to a particular class. Since we approach this problem through the lens of statistical testing, we first need to (i) determine whether there is any difference in the distances from the classes present in the local neighborhood; and if such a difference exists (ii) investigate the distances pairwise between classes to determine the dominating class(es).

For (i), we perform a one-way Welch ANOVA study with null hypothesis  $H_0 : \hat{\boldsymbol{\mu}}_{\hat{y}=1} = \hat{\boldsymbol{\mu}}_{\hat{y}=2} = \dots = \hat{\boldsymbol{\mu}}_{\hat{y}=C}$  at significance level  $\alpha$ , which if rejected, proves that there is at least one class that is on average closer (or farther) to  $\tilde{\mathbf{x}}$  at layer  $\lambda$ . Here  $\hat{\boldsymbol{\mu}}_{\hat{y}=i}$  are the distances to the closest validation points from class  $i$ . For (ii), i.e. to find which class is the closest and by how much, we must perform additional post-hoc tests. We propose to employ a pair-wise  $t$ -testing setup between all the distances from the classes present in  $\hat{\mathbf{y}}$ . If  $C'$ -many distinct classes are present in  $\hat{\mathbf{y}}$ , then we carry out  $\binom{C'}{2}$  pairwise comparisons between class distances. Given a distance vector from class  $c_1$ ,  $\hat{\boldsymbol{\mu}}_{\hat{y}=c_1}$ , and a distance vector from class  $c_2$ ,  $\hat{\boldsymbol{\mu}}_{\hat{y}=c_2}$ , we set up a null hypothesis  $H_0 : \hat{\boldsymbol{\mu}}_{\hat{y}=c_1} \leq \hat{\boldsymbol{\mu}}_{\hat{y}=c_2}$  stating that the mean class distance of class  $c_2$  is greater or equal than the mean class distance of class  $c_1$ . We also establish the corresponding alternative  $H_1 : \hat{\boldsymbol{\mu}}_{\hat{y}=c_1} > \hat{\boldsymbol{\mu}}_{\hat{y}=c_2}$  under which the mean class distance of class  $c_2$  is strictly smaller than the mean class distance of class  $c_1$ . A significant result therefore implies that the test data point  $\tilde{\mathbf{x}}$  is closer to  $c_2$  than to  $c_1$ . Carrying out this testing procedure for all pair-wise combination of classes yields a matrix  $\mathbf{P} \in [0, 1]^{C' \times C'}$  containing all  $p$ -values for the respective pair-wise tests.

In addition to  $p$ -values, the performed  $t$ -tests also returns an effect size for all combinations of classes tested. For a class pair  $c_1, c_2$  the effect size quantifies the magnitude of the difference between two groups and is defined as  $e = \frac{\hat{\boldsymbol{\mu}}_{\hat{y}=c_1} - \hat{\boldsymbol{\mu}}_{\hat{y}=c_2}}{\sigma}$  where  $\sigma$  is estimated from  $\hat{\boldsymbol{\mu}}_{\hat{y}=c_2}$ . Similar as with  $p$ -values, we collect the effect sizes in a matrix  $\mathbf{E} \in \mathbb{R}^{C' \times C'}$ .

### 3.3 Aggregation of p-values

Performing the pair-wise statistical hypothesis testing procedure for each layer yields a collection of matrices  $\{\mathbf{P}_\lambda\}_{\lambda=1}^L, \{\mathbf{E}_\lambda\}_{\lambda=1}^L$  that can be combined into tensors  $\mathcal{P}, \mathcal{E}$  for the  $p$ -value and effect sizes, respectively. Our final goal being to obtain a vector of  $p$ -values signaling the support strength for each class, we devise an aggregation scheme through multiple hypothesis testing correction and averaging.

First, we need to ensure that our false positive rate is not inflated due to carrying out multiple tests on the same data. Thus, we apply a two stage false discovery rate correction on top of the  $p$ -value tensor  $\mathcal{P}$  which enables us to bound incorrect rejections of the null.

Next, we start aggregating  $p$ -values across layers, i.e. we compute a single  $p$ -value for a fixed combination of classes  $c_1$  and  $c_2$  based on the full  $p$ -value tensor  $\mathcal{P}$ . We do that by calculating the arithmetic mean over the collection of  $p$ -values between class  $c_1$  and  $c_2$  and multiplying the resulting mean by 2, or for a weighted average with weights  $\mathbf{w}$ , the multiplicative factor is  $\min(2, \frac{1}{\max(\mathbf{w})})$ . If an averaged  $p$ -value is larger than 1 after aggregation, we clip it to 1. This particular choice of aggregation is supported by [Vovk and Wang \(2019\)](#), which states that  $p$ -values can be averaged independent of their dependence structure. While [Vovk and Wang \(2019\)](#) presents a general framework supporting multiple different mean computations,

the (weighted) arithmetic averaging method is preferred in cases of strong  $p$ -value dependence (which we typically expect between latent neural network representations).

Having now obtained a matrix of  $p$ -values, we still have to aggregate across one of the classes dimensions. Since our hypothesis testing setup yields significant results if the column class has smaller mean distance, we aggregate across columns instead of rows. The aggregation is performed identical to the previous stage: we compute the arithmetic mean across columns and multiply the result by 2. In addition to  $\mathcal{P}$ , we also aggregate the effect sizes  $\mathcal{E}$  into a single vector. Since effect sizes do not need to abide by strict aggregation rules dictating the consistency of the final aggregation (as was the case with  $p$ -values), we simply compute the arithmetic mean across layers and class columns without needing to apply any correction factor.

### 3.4 Prediction based on significant $p$ -value

The final aggregation result is a vector of  $p$ -values  $\mathbf{p} \in [0, 1]^C$  and a vector of effect sizes  $\mathbf{e} \in \mathbb{R}^C$ . To make a classification decision for  $\tilde{\mathbf{x}}$ , we query  $\mathbf{p}$  for the minimum  $p$ -value  $\tilde{p} = \min \mathbf{p}$  and the index of the maximum effect size  $\tilde{y} = \arg \max \mathbf{e}$ . If the minimum  $p$ -value  $\tilde{p}$  happens to be significant (i.e. below a chosen significance level  $\alpha$ ), then we return the index  $\tilde{y}$  as the classification result. However, if no single  $p$ -value in  $\mathbf{c}$  happens to be significant, then we abstain (i.e. return  $\perp$ ). Note that  $p$ -values are being used to determine whether we should reject or accept  $\tilde{\mathbf{x}}$ , while the effect sizes determine the classification result for an accepted test sample. This separation of concerns allows us to also make a confident classification decision in case multiple  $p$ -values in  $\mathbf{p}$  fall below our significance level  $\alpha$ .

### 3.5 Distance computation to convex hull

The proposed method allows us to correctly classify inputs that are supported by sufficient evidence from one specific class  $\tilde{y}$  or to abstain from prediction in case there is a large amount of disagreement in the local neighborhood around the test input  $\tilde{\mathbf{x}}$ . However, some OOD data points might lie far from the density defined by the validation points  $\{\mathbf{X}_\lambda\}_{\lambda=1}^L$  but at the same time be closest to one particular class. To detect this type of OOD data as well, we propose to additionally validate the distance of a test input to the predicted class  $\tilde{y}$ . Concretely, we compute the convex hull of the predicted class and reject a data point if its distance from the convex hull exceeds a pre-calibrated maximum threshold  $\gamma$ .

## 4 Theoretical Connections & Analysis

We pursue two goals in our extended classification scenario. First, we want to make sure that we do not produce overconfident classification decisions. We call this step the **Selection-step**, or **S-step** for short. The S-step helps us avoid OOD and adversarial sample classification. Second, we want to make sure we produce

---

### Algorithm 1 $p$ -DkNN prediction algorithm

---

**Input:** Test point:  $\tilde{\mathbf{x}}$ , test point activations:  $\{\tilde{\mathbf{x}}_\lambda\}_{\lambda=1}^L$ , validation activations:  $\{\mathbf{X}_\lambda\}_{\lambda=1}^L$ , validation labels:  $\mathbf{y}$ , number of neighbors:  $k$ , significance level:  $\alpha$ , max convex hull distance:  $\gamma$ .

**Output:** Classification  $\tilde{y} \in [C]$  or abstain  $\perp$

```

1 for  $\lambda \in [L]$  do
2    $\boldsymbol{\mu} \leftarrow \text{get\_distances}(\mathbf{X}_\lambda, \tilde{\mathbf{x}}_\lambda)$ 
3    $\hat{\boldsymbol{\mu}}, i \leftarrow \text{get\_smallest}(\boldsymbol{\mu}, k)$ 
4    $\hat{\mathbf{y}} \leftarrow \text{get\_classes}(\mathbf{y}, i)$ 
5    $e_{\text{anova}}, p_{\text{anova}} \leftarrow \text{anova}(\hat{\boldsymbol{\mu}}, \hat{\mathbf{y}})$ 
6   if  $p_{\text{anova}} < \alpha$  then
7      $\mathcal{E}_\lambda, \mathcal{P}_\lambda \leftarrow \text{pairwise\_t}(\boldsymbol{\mu}, \hat{\mathbf{y}})$ 
8   else
9      $\mathcal{P}_\lambda \leftarrow \text{fill\_with}(p_{\text{anova}})$ 
10     $\mathcal{E}_\lambda \leftarrow \text{fill\_with}(e_{\text{anova}})$ 
11  end
12 end
13  $\mathcal{P} \leftarrow \text{correct\_mult\_test}(\mathcal{P}, \alpha)$ 
14  $\mathbf{p} \leftarrow \text{aggregate\_p}(\mathcal{P})$ 
15  $\mathbf{e} \leftarrow \text{aggregate\_e}(\mathcal{E})$ 
16  $\tilde{p} \leftarrow \min(\mathbf{p}); \tilde{y} \leftarrow \text{argmax}(\mathbf{e})$ 
17 if  $\tilde{p} < \alpha$  then
18    $\mathbf{c} \leftarrow \text{conv\_hulls}(\{\mathbf{X}_\lambda\}_{\lambda=1}^L, \tilde{y})$ 
19   if  $\text{are\_in\_ch}(\{\tilde{\mathbf{x}}_\lambda\}_{\lambda=1}^L, \mathbf{c}, \gamma)$  then
20     return  $\tilde{y}$ 
21   end
22 end
23 return  $\perp$ 

```

---

Table 1: **Confusion Matrix for the Extended Binary Classification Scenario.** Selection, Classification, and Type I and II errors are marked.

| Dec \ True | $\top, 0$ | $\top, 1$ | $\perp, 0$ | $\perp, 1$ |
|------------|-----------|-----------|------------|------------|
| $\top, 0$  | ✓         | × (C-II)  |            |            |
| $\top, 1$  | × (C-I)   | ✓         |            | S-I        |
| $\perp, 0$ |           |           |            |            |
| $\perp, 1$ |           | S-II      |            | ✓          |

accurate classification decisions for samples that we accept in the S-step. We denote this as the **Classification step**, or **C-step**. The C-step is akin to empirical loss minimization, as is common in statistical learning. The S-step is always a binary decision, regardless of the number of classes in the target problem (C-step). To simplify our theoretical formulation and analysis, we consider a binary classification scenario for the C-step, too. Table 1 shows the confusion table for our extended setup. Due to the nature of our problem setup, the S-step conceptually precedes the C-step, *i.e.*, if a sample is OOD without a doubt (*e.g.*, from the preceding  $S$  distribution) then classifying it would produce a vacuous decision regardless of the fact that the calculated label matches a ground-truth label, or not.

**NP-Classification and NP-ERM Formulation** In the classification step, we care most about the classification accuracy; or minimizing the risk  $R(h) = \mathbb{E}[\mathbb{1}_{[h(x) \neq y]}] = \mathbb{P}[h(x) \neq y]$  which is the weighted sum of type I and type II errors:  $R(h) = \mathbb{P}[Y = 0]R_0(h) + \mathbb{P}[Y = 1]R_1(h)$ . As we previously discussed, for a safety-critical classifier, in the selection step, it is essential that the type I error (that is, probability of classifying OOD samples as ID) be bounded and thus a NP-Classification scenario is more appropriate. Therefore, we formulate our setup in an NP-ERM setting (Scott and Nowak):

Let  $h \in \mathcal{H}$  be a trained model hypothesis,  $x \in \mathcal{X} \subseteq \mathbb{R}^d$  our test input,  $\mathcal{Y} = \{0, 1\}$  the space of C-step ground truth labels, and  $\mathcal{Z} = \{\perp, \top\}$  the space of S-step ground truth labels. We define  $f(x) = (m(x), h(x)) \rightarrow \{\perp, \top\} \times \{0, 1\}$  as the extended classifier’s decision function which uses the aggregated  $p$ -values for class  $c \in \mathcal{Y}$ :  $\underline{p}_c(x) = (p_{c,1}, \dots, p_{c,L})^T$  to determine the the selected samples. The corresponding effect sizes  $\underline{es}_c(x) = (es_{c,1}, \dots, es_{c,L})^T$  are used in the classification step. We formulate our approach as the following optimization problem:

$$\arg \min_{\mathbf{w} \in \Delta(L), \omega \in [0,1]} \frac{\omega}{n} \sum_{x \in \mathcal{X}} \mathbb{1}_{[m(x)=\perp, z=\top]} + \frac{1-\omega}{|\{m(x)=\top\}|} \sum_{m(x)=\top} \mathbb{1}_{[h(x) \neq y]} \quad (1)$$

such that

$$\frac{1}{n} \sum_{x \in \mathcal{X}} \mathbb{1}_{[m(x)=\top, z=\perp]} < \alpha + \epsilon \quad (2)$$

$$\frac{1}{|\{m(x)=\top\}|} \sum_{m(x)=\top} \mathbb{1}_{[h(x)=1, y=0]} < \alpha + \epsilon \quad (3)$$

$$m(x) = \begin{cases} \top & \langle \mathbf{w}, \underline{p}_0(x) \rangle < \alpha + \epsilon \vee \\ & \langle \mathbf{w}, \underline{p}_1(x) \rangle < \alpha + \epsilon \\ \perp & \text{otherwise} \end{cases} \quad (4)$$

$$h(x) = \arg \max_{c \in \mathcal{Y}=\{0,1\}} \langle \mathbf{w}, \underline{es}_c(x) \rangle \quad (5)$$

In (1), we are minimizing the weighted loss of type II error in the S-step (*i.e.*, rejecting an ID sample) and the misclassification of the C-step. Weights  $\mathbf{w}$  are on the  $L$ -dimensional probability simplex  $\Delta(L)$ .  $\omega \in [0, 1]$

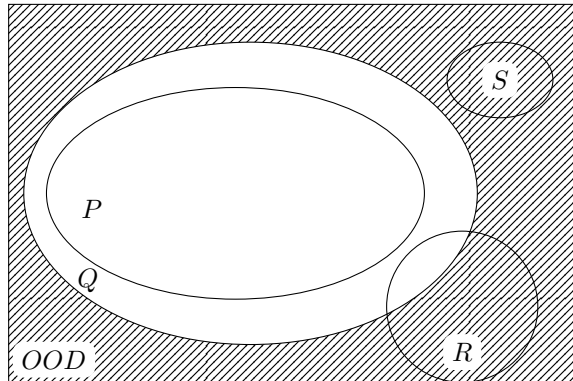
Table 2: **Experimental results on synthetic Gaussians with  $p$ -DkNN and competing methods.** For in-distribution data (**gauss**), we align the percentage of accepted samples to 0.965 and report the classification accuracy. For test-time data (**g\_1**, **g\_2**, **g\_3**), we only report the ratio of accepted samples. Up arrows ( $\uparrow$ ) indicates that higher rates are better, down arrows ( $\downarrow$ ) indicates that lower rates are better, right arrows ( $\rightarrow$ ) indicates that a balanced rate (0.5) is best.

| Model                              | gauss |                         | g_1                     | g_2                     | g_3                        |
|------------------------------------|-------|-------------------------|-------------------------|-------------------------|----------------------------|
|                                    | Pass  | Acc                     | Pass                    | Pass                    | Pass                       |
| NN (Hendrycks and Gimpel, 2016)    | 0.965 | <b>0.997</b> $\uparrow$ | 1.0 $\downarrow$        | 0.915 $\downarrow$      | 0.496 $\rightarrow$        |
| DkNN (Papernot and McDaniel, 2018) | 0.965 | 0.996 $\uparrow$        | 1.0 $\downarrow$        | 0.999 $\downarrow$      | 0.751 $\rightarrow$        |
| ReBeL (Raghuram et al., 2020)      | 0.965 | 0.991 $\uparrow$        | 0.975 $\downarrow$      | 0.871 $\downarrow$      | 0.667 $\rightarrow$        |
| Trust (Jiang et al., 2018)         | 0.965 | N/A                     | 0.04 $\downarrow$       | 0.005 $\downarrow$      | 0.533 $\rightarrow$        |
| $p$ -DkNN                          | 0.965 | <b>0.997</b> $\uparrow$ | <b>0.0</b> $\downarrow$ | <b>0.0</b> $\downarrow$ | <b>0.498</b> $\rightarrow$ |

is a hyper-parameter that helps us tune this trade-off. Since we are operating in an NP hypothesis testing framework, both the S-step and the C-step type I errors are bounded per (2) and (3) with slack parameter  $\epsilon$ . Equation (4) represents the selection step via the meta-hypothesis test  $\langle \mathbf{w}, \mathbf{p} \rangle < \alpha$ , where  $\mathbf{w}$  are the weights assigned to each layer. Finally, (5) chooses the class with largest effect size (C-step). It is possible that after the S-step, the accepted samples show exclusive evidence for only one class; in that case, the C-step and (5) are trivial.

### What constitutes OOD & Connection to PQ-Learning (Goldwasser et al., 2020)

The OOD precise definition (*i.e.*, what is *not* in-distribution) is elusive. If the underlying task and data distribution are non-overlapping ( $S$ ), the question is settled. However, some OOD samples (such as adversarial examples) are very close to actual ID samples ( $R$ ) such that, for example, in the absence of semantic changes, a human can predict the true label despite the adversarial noise. On the other end of the spectrum, there is no question that clean training samples ( $P$ ) are ID. However, it is considered beneficial for classifiers to be robust against distribution shifts ( $Q$ ) and generalize beyond their training sets. Most



works in anomaly detection and/or robust classification are different in how they define what is an appropriate definition for  $Q$ , *i.e.*, the distribution (or set) of samples that should be classified at test (inference) time. Importantly, these approaches also differ in how they define  $Q$ . Goldwasser et al. directly work with samples  $\tilde{x} \sim Q$  and present two algorithms given labels are present for  $\tilde{x}$  or not. If we let  $S = \{x | m(x) = \top\}$  and  $\omega = 1/2$ , our empirical loss function in (1) is similar to that of a PQ-learner. The key difference is that PQ-learners studied in Goldwasser et al. (2020) do not have bounded type I error in their selection step.

Note that for ease of presentation, in (1), we defined  $Q$  by the ground truth membership labels  $z$ . However, in our method in §3, we do not require such explicit labels. Instead, the choice of distance metric, the  $k$ -nearest neighbor graph in each layer, the choice of standard hypothesis tests, and the aggregation method implicitly dictate our effective  $Q$  distribution.

## 5 Empirical Evaluation

**Gaussians** We first want to determine how well  $p$ -DkNN handles various types of carefully crafted (potentially OOD) test-time inputs and how specifically OOD decisions are being made by  $p$ -DkNN. To do so, we evaluate our approach on a synthetic dataset consisting of three two-dimensional Gaussian blobs:

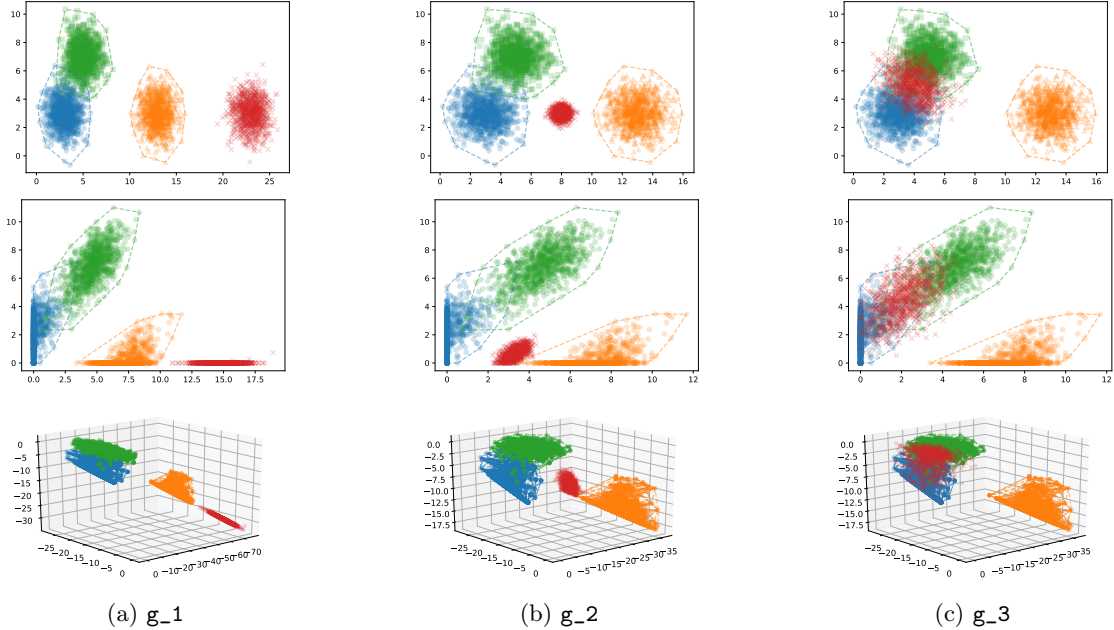


Figure 3: **Neural network representations for our gauss datasets.** Circles  $\circ$  ( $g_1$ ), triangles  $\triangle$  ( $g_2$ ), and squares  $\square$  ( $g_3$ ) show ID training data, while crosses  $\times$  show (potentially OOD) test-time inputs. The first row depicts the input space for the three datasets, the second row the first hidden layer, and the third row the log-softmax output. Dashed lines are the convex hulls.

$g_1 \sim \mathcal{N}([3 \ 3]^T, \mathbf{I})$ ,  $g_2 \sim \mathcal{N}([13 \ 3]^T, \mathbf{I})$ ,  $g_3 \sim \mathcal{N}([5 \ 7]^T, \mathbf{I})$ . We train a neural network classifier consisting of a single fully-connected two-dimensional latent layer and a fully-connected three-dimensional log-softmax output layer using 1000 samples from each Gaussian and achieve 98.80% accuracy on this task. This network can be used as a stand-alone classifier or can be augmented using  $p$ -DkNN’s inference procedure.

To test the rejection rate and accuracy of  $p$ -DkNN we generate four test sets: (i) **gauss** consisting of in-distribution data points from Gaussians  $g_1$ ,  $g_2$ , and  $g_3$ , a clear ID dataset; (ii) **g\_1** consisting of data points sampled from  $\mathcal{N}([23 \ 3]^T, \mathbf{I})$ , a clear OOD dataset; (iii) **g\_2** consisting of data points sampled from  $\mathcal{N}([8 \ 3]^T, 0.1\mathbf{I})$ , another OOD dataset; and (iv) **g\_3** consisting of data points sampled from  $\mathcal{N}([4 \ 5]^T, \begin{bmatrix} 1 & -0.2 \\ -0.2 & 1 \end{bmatrix})$ , a dataset that is designed to spread its density equally between the intersection of  $g_1$  and  $g_2$  (a region of high classification uncertainty) and the individual clusters  $g_1$  and  $g_2$  (regions of low classification uncertainty). All datasets, including their neural network activations, are shown in Figure 3.

We report our results in detail in Table 2. In addition to thresholding the underlying neural network (Hendrycks and Gimpel, 2016) and applying DkNN on top of the underlying neural network, we also compare against two recent related OOD detection techniques: REBEL (Raghuram et al., 2020) and TRUST (Jiang et al., 2018). We clearly see that competing approaches are outperformed by  $p$ -DkNN on all datasets.

In addition to the acceptance rate of and the accuracy on samples, we also analyze the rejection reason for rejected data points for  $p$ -DkNN. For **gauss** and **g\_3**, i.e. datasets that completely lie within the support of the trained distribution, all rejections happen because of inconclusive  $p$ -values. On the other hand, all rejections are determined by an exceeded distance to the convex hull of the nearest cluster for **g\_1**. **g\_2**, a dataset that is positioned exactly between the three in-distribution Gaussians, strikes a middle-ground as 53% of rejections happen because of inconclusive  $p$ -values (data points close to the mode of the Gaussian) while 47% of rejections can be attributed to the convex hull criterion (data points in the tail of the Gaussian).

**Evaluation on Standard Datasets** Our method  $p$ -DkNN builds upon DkNN. Thus, we evaluate  $p$ -DkNN against DkNN as well as standard neural networks (NN) in Table 3. We use MNIST, FashionMNIST, SVHN, and GTSRB datasets as clean samples. We test the methods on out-of-distribution (OOD), rotated samples, and adversarial examples found with a feature-based adaptive attack (Sabour et al., 2016) denoted

Table 3: **Performance Comparison** between standard NN (Neural Network) architecture, DkNN and  $p$ -DkNN.  $\uparrow$  higher is better,  $\downarrow$  lower is better, otherwise not applicable. Pairs of OOD data (OOD-1, OOD-2) for: MNIST (NotMNIST, FashionMNIST), FashionMNIST (NotMNIST, MNIST), SVHN (CIFAR10, GTSRB), GTSRB (CIFAR10, SVHN). Rotated samples are denoted as  $\angle 45$ . We report the rate of examples that passed the threshold (*Pass*) and their accuracy (*Acc*) (on the accepted examples). The results are aligned according to *Pass* on the clean samples (Attack None). Exact hyperparameter choices for all methods are documented in Section B.

| ATTACK      | MODEL     | MNIST                    |                        | FASHIONMNIST             |                        | SVHN                     |                        | GTSRB                    |                        |
|-------------|-----------|--------------------------|------------------------|--------------------------|------------------------|--------------------------|------------------------|--------------------------|------------------------|
|             |           | PASS                     | ACC                    | PASS                     | ACC                    | PASS                     | ACC                    | PASS                     | ACC                    |
| NONE        | NN        | <u>.956</u> $\uparrow$   | <b>.998</b> $\uparrow$ | <u>.908</u> $\uparrow$   | .945 $\uparrow$        | <u>.900</u> $\uparrow$   | .949 $\uparrow$        | <u>.900</u> $\uparrow$   | .928 $\uparrow$        |
|             | DkNN      | <u>.956</u> $\uparrow$   | .996 $\uparrow$        | <b>.909</b> $\uparrow$   | .936 $\uparrow$        | <u>.892</u> $\uparrow$   | <b>.951</b> $\uparrow$ | <u>.900</u> $\uparrow$   | <b>.979</b> $\uparrow$ |
|             | $p$ -DkNN | <u>.956</u> $\uparrow$   | <b>.998</b> $\uparrow$ | <u>.908</u> $\uparrow$   | <b>.946</b> $\uparrow$ | <u>.900</u> $\uparrow$   | .944 $\uparrow$        | <u>.888</u> $\uparrow$   | .970 $\uparrow$        |
| OOD-1       | NN        | .200 $\downarrow$        | .104                   | .774 $\downarrow$        | .150                   | .521 $\downarrow$        | .093                   | <b>.169</b> $\downarrow$ | .004                   |
|             | DkNN      | .235 $\downarrow$        | .163                   | .414 $\downarrow$        | .283                   | <b>.322</b> $\downarrow$ | .090                   | .281 $\downarrow$        | .001                   |
|             | $p$ -DkNN | <b>.182</b> $\downarrow$ | .154                   | <b>.405</b> $\downarrow$ | .257                   | .375 $\downarrow$        | .094                   | .269 $\downarrow$        | .004                   |
| OOD-2       | NN        | <b>.068</b> $\downarrow$ | .047                   | .748 $\downarrow$        | .130                   | .545 $\downarrow$        | .034                   | <b>.214</b> $\downarrow$ | .003                   |
|             | DkNN      | .300 $\downarrow$        | .034                   | .441 $\downarrow$        | .148                   | <b>.330</b> $\downarrow$ | .017                   | .309 $\downarrow$        | .003                   |
|             | $p$ -DkNN | .170 $\downarrow$        | .042                   | <b>.161</b> $\downarrow$ | .263                   | .362 $\downarrow$        | .020                   | .287 $\downarrow$        | .003                   |
| FEAT        | NN        | <b>.0</b> $\downarrow$   | .0                     | .471 $\downarrow$        | .0                     | .702 $\downarrow$        | .0                     | <b>.362</b> $\downarrow$ | .0                     |
|             | DkNN      | .442 $\downarrow$        | .732                   | .716 $\downarrow$        | .523                   | .686 $\downarrow$        | .373                   | .516 $\downarrow$        | .102                   |
|             | $p$ -DkNN | .161 $\downarrow$        | .133                   | <b>.389</b> $\downarrow$ | .146                   | <b>.571</b> $\downarrow$ | .303                   | .452 $\downarrow$        | .142                   |
| FGSM        | NN        | .680 $\downarrow$        | .022                   | .933 $\downarrow$        | .095                   | .828 $\downarrow$        | .042                   | .489 $\downarrow$        | .094                   |
|             | DkNN      | .373 $\downarrow$        | .149                   | .672 $\downarrow$        | .398                   | <b>.485</b> $\downarrow$ | .046                   | .417 $\downarrow$        | .199                   |
|             | $p$ -DkNN | <b>.239</b> $\downarrow$ | .102                   | <b>.589</b> $\downarrow$ | .170                   | .502 $\downarrow$        | .039                   | <b>.379</b> $\downarrow$ | .191                   |
| PGD         | NN        | .999 $\downarrow$        | .010                   | 1.00 $\downarrow$        | .061                   | 1.00 $\downarrow$        | .030                   | 1.00 $\downarrow$        | .012                   |
|             | DkNN      | .646 $\downarrow$        | .014                   | .693 $\downarrow$        | .164                   | .946 $\downarrow$        | .030                   | .850 $\downarrow$        | .018                   |
|             | $p$ -DkNN | <b>.518</b> $\downarrow$ | .016                   | <b>.575</b> $\downarrow$ | .098                   | <b>.929</b> $\downarrow$ | .031                   | <b>.826</b> $\downarrow$ | .016                   |
| $\angle 45$ | NN        | <b>.399</b> $\downarrow$ | .816                   | .675 $\downarrow$        | .140                   | .535 $\downarrow$        | .351                   | .556 $\downarrow$        | .180                   |
|             | DkNN      | .439 $\downarrow$        | .788                   | <b>.251</b> $\downarrow$ | .353                   | <b>.165</b> $\downarrow$ | .362                   | .572 $\downarrow$        | .197                   |
|             | $p$ -DkNN | .440 $\downarrow$        | .846                   | .307 $\downarrow$        | .243                   | .273 $\downarrow$        | .359                   | <b>.502</b> $\downarrow$ | .212                   |

as *Feat* (details below), PGD (Madry et al., 2018), and FGSM (Goodfellow et al., 2014), with max distortion  $\varepsilon = 0.3$  on MNIST and FashionMNIST, and  $\varepsilon = 0.03$  on SVHN and GTSRB.

The aggregation of  $p$ -values is conservative and in practice requires us to weight the values from each layer differently. Frosst et al. (2019) showed that there is a high entanglement in all layers apart from the last one. We use this result as our guidance in the selection of weights per layer. We weight the  $p$ -values based on the layers they come from and average them to reduce their magnitude.

The feature attack is a natural choice for DkNN and  $p$ -DkNN: it optimizes for a minimal perturbation that moves an internal representation of a clean sample close to an adversarial representation (from another example called the *guide*). Feature adversarial examples against DkNN and  $p$ -DkNN usually draw the adversarial digit in the background, which is clearly visible in most cases (see an example in Figure 4). This confirms previous findings (Sitawarin and Wagner, 2019, 2020). The feature attack is not optimal for vanilla DNNs, where adversarial examples optimizing over the model’s output work better (e.g., FGSM, PGD, etc.). For both, MNIST and GTSRB we observe that NN rejects most of the feature adversaries by significantly lowering its confidence.



Figure 4: **Feature attack** with digit 3 for the digit 7 against  $p$ -DkNN.

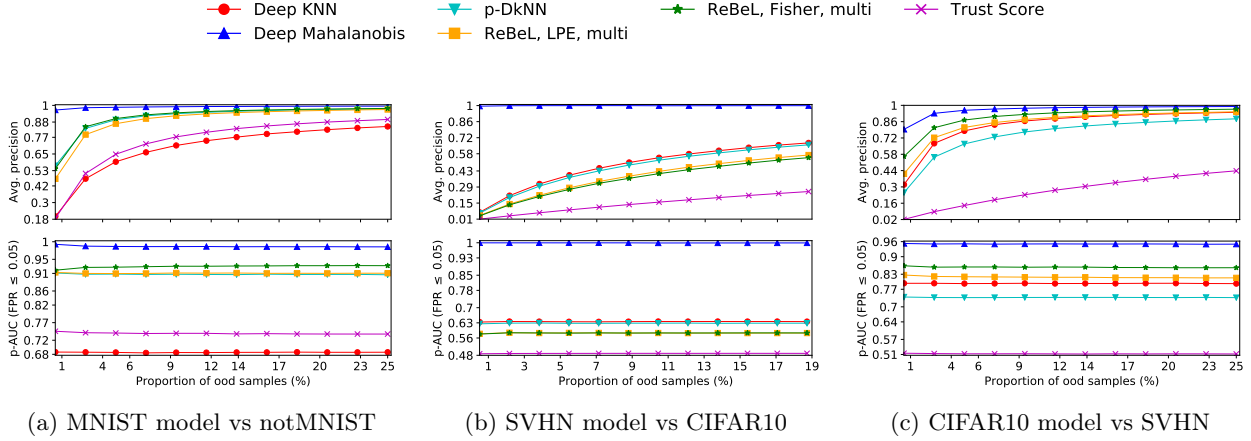


Figure 5: OOD detection performance comparison between  $p$ -DkNN and other methods.

**Comparison with ReBeL and Trust** We also compare  $p$ -DkNN against other unsupervised methods such as ReBeL (Raghuram et al., 2020) and Trust (Jiang et al., 2018). During said comparison, we adhere to their choice of basic parameters, such as the number of nearest neighbors  $k$ , which is given by a heuristic  $k = \lceil n^{0.4} \rceil$ , model architecture, and the tuning of hyper-parameters on the training set, where we adjust the  $p$ -value for  $p$ -DkNN. This allows for a fair comparison between the methods.

For this comparison, we use all the components from our main method apart from the convex hulls and we find neighbors on the training set instead of the validation set. We present the adjusted method as Algorithm 2. For the correction of  $p$ -values, we use the two stage fdr correction (non-negative), denoted as *fdr\_tsbh*. We tune the weights per layer that are used for a weighted mean of the  $p$ -values and effect sizes. We find that for smaller networks, for instance, architectures used for MNIST or SVHN datasets with 2, 3 or 4 convolutional layers followed by 1 or 2 fully connected layers, it is beneficial to put more weight on the last layer. For larger networks, such as ResNet-34 used for CIFAR10, the larger weights should be assigned to final layers (not only the last one).

First, we analyze the performance of  $p$ -DkNN against other methods for OOD data. Our experiments in Figure 5a on MNIST show that  $p$ -DkNN is on-par with ReBeL and outperforms other unsupervised methods (e.g., Trust Score). The Deep Mahalanobis (Lee et al., 2018) method is supervised

---

**Algorithm 2**  $p$ -DkNN prediction algorithm for the comparisons within the ReBeL framework.

---

**Input:** Test point:  $\tilde{\mathbf{x}}$ , test point activations:  $\{\tilde{\mathbf{x}}_\lambda\}_{\lambda=1}^L$ , activations from the training set:  $\{\mathbf{X}_\lambda\}_{\lambda=1}^L$ , labels from the training set:  $\mathbf{y}$ , number of neighbors:  $k$ , significance level:  $\alpha$ .

**Output:** Classification  $\tilde{y} \in [C]$  or abstain  $\perp$

```

24  $\mathcal{P} \leftarrow \text{initialize\_pvalues}()$ 
25  $\mathcal{E} \leftarrow \text{initialize\_effect\_sizes}()$ 
26 for  $\lambda \in [L]$  do
27    $\boldsymbol{\mu} \leftarrow \text{get\_distances}(\mathbf{X}_\lambda, \tilde{\mathbf{x}}_\lambda)$ 
28    $\hat{\boldsymbol{\mu}}, \text{indices} \leftarrow \text{get\_smallest}(\boldsymbol{\mu}, k)$ 
29    $\hat{\mathbf{y}} \leftarrow \text{get\_classes}(\mathbf{y}, \text{indices})$ 
30    $p_{\text{anova}} \leftarrow \text{anova}(\hat{\boldsymbol{\mu}}, \hat{\mathbf{y}})$ 
31   if  $p_{\text{anova}} < \alpha$  then
32      $\mathcal{P}_\lambda \leftarrow \text{pairwise\_t}(\boldsymbol{\mu}, \hat{\mathbf{y}})$ 
33      $\mathcal{E}_\lambda \leftarrow \text{effect\_size\_hedges}(\boldsymbol{\mu}, \hat{\mathbf{y}})$ 
34   end
35 end
36  $\mathcal{P} \leftarrow \text{correct\_mult\_test}(\mathcal{P}, \alpha)$ 
37  $\mathbf{p} \leftarrow \text{aggregate\_p}(\mathcal{P})$ 
38  $\mathbf{e} \leftarrow \text{aggregate\_e}(\mathcal{E})$ 
39  $\tilde{y} \leftarrow \text{argmax}(\mathbf{e})$ 
40  $\tilde{p} \leftarrow \mathbf{p}[\tilde{y}]$ 
41 if  $\tilde{p} < \alpha$  then
42   return  $\tilde{y}$ 
43 end
44 return  $\perp$ 

```

---

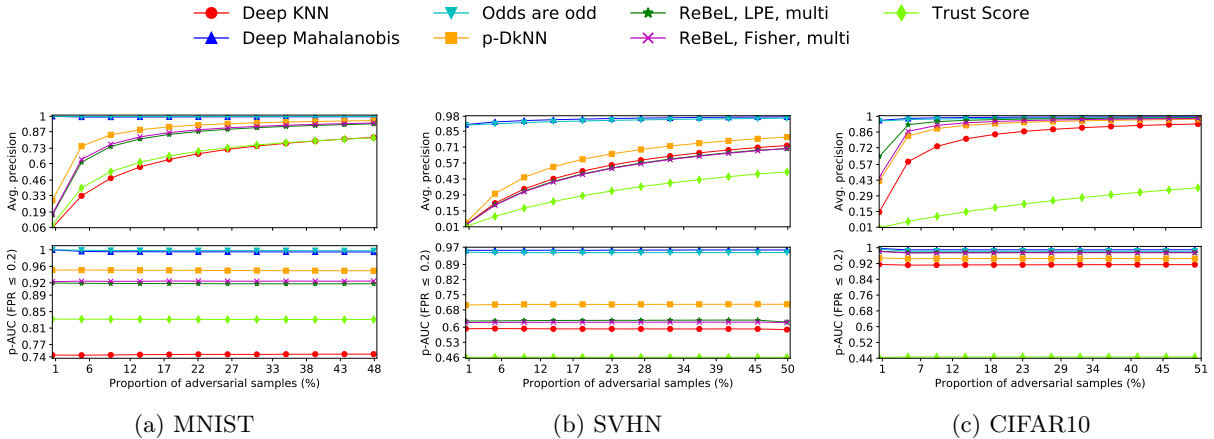


Figure 6: PGD adversarial sample detection performance comparison between  $p$ -DkNN and other methods.

so it clearly performs better than the unsupervised methods. Then, for the SVHN dataset in Figure 5b,  $p$ -DkNN is on par with DkNN and both methods are clearly better than other unsupervised ones. Finally, for CIFAR10 in Figure 5c,  $p$ -DkNN is slightly worse than ReBeL and DkNN but still performs much better than the Trust Score.

Second, for the adversarial examples found using the PGD attack,  $p$ -DkNN is the best performing method for both MNIST (Figure 6a) and SVHN (Figure 6b) datasets. For the CIFAR10 dataset (Figure 6c), our method is on par with ReBeL and outperforms other unsupervised methods. The Deep Mahalanobis and Odds are Odd methods are both supervised and clearly outperform the unsupervised methods. The Odds are Odd method targets specifically the adversarial examples, hence it is not applied to the OOD detection.

Overall, we find that  $p$ -DkNN provides the best performance in most cases.

## 6 Limitations

Due to our bounds on type I error,  $p$ -DkNN is a conservative approach. The tight control on type I error is the bedrock of the hypothesis testing framework. Consequently, most techniques and considerations we delineated in Section 3—such as employing ANOVA tests, p-value corrections, and the use of a separate validation set to estimate representational distances—are meant to keep the type I error in check. However, as we demonstrated pictorially in Figure 1 (d), a strict control on type I error would necessarily mean an increase in type II error (and by extension the total error rate). Both prior work (Raghuram et al., 2020) and our empirical study have verified this observation: if we applied all the said techniques, then many of our in-distribution samples are rejected.<sup>2</sup> For instance, on MNIST where the classification accuracy on the clean inputs is around 99%, a stringent variant of our method can reject 10% of in-distribution samples. This might be prohibitive in some applications. This motivated us to systematically loosen the aforementioned constraints. We based this study off of the established framework of NP-classification and our formulation of the problem in Section 4 contains all such considerations. In our empirical study, we found that weighting the  $p$ -values and effect sizes such that deeper layers are weighted more to balance an effective trade-off.

The requirement to employ a separate moderately-sized validation set at inference may also not be practical for certain applications and datasets of limited size. In the machine learning literature, usually a smaller fraction of the training set is used for validation and hyper-parameter tuning. However in  $p$ -DkNN, this assumption ensures that test statistics are independent across the layers. Moreover, it allow us to

<sup>2</sup>We like to re-iterate the point we made in Section 4 that the definition of OOD (and thus ID) is an elusive concept. Indeed, almost all practical datasets contain so-called outliers for the same reason.

properly model the decision boundaries found on the training set. In practice, this assumption can also be relaxed (as have been in prior work (Raghuram et al., 2020)) which is what we also did in parts of our empirical study.

## 7 Conclusions

We presented  $p$ -DkNN, a method for detecting out-of-distribution inputs at test time given an already trained neural network classifier. To provide grounded estimates of uncertainty, our approach analyzes internal layer representations with statistical hypothesis testing. Our approach is best studied in a Neyman-Pearson classification setup. We also positioned it with respect to recent work in selective classification with arbitrarily distributed inputs at inference. Our evaluation on both synthetic and standard datasets shows superior performance to recent proposals in the literature. Among the many directions for future work, we are particularly interested in the benefits of composing the  $p$ -values associated with the predictions of different neural networks (e.g., when these networks operate on different modalities of the same input).

## Acknowledgements

We would like to acknowledge our sponsors, who support our research with financial and in-kind contributions: CIFAR through the Canada CIFAR AI Chair program, DARPA through the GARD program, Intel, Meta, NFRF through an Exploration grant, and NSERC through the Discovery Grant and COHESA Strategic Alliance. Resources used in preparing this research were provided, in part, by the Province of Ontario, the Government of Canada through CIFAR, and companies sponsoring the Vector Institute. We would like to thank members of the CleverHans Lab for their feedback.

## References

- Dario Amodei, Chris Olah, Jacob Steinhardt, Paul Christiano, John Schulman, and Dan Mané. Concrete problems in ai safety. *arXiv preprint arXiv:1606.06565*, 2016.
- Hyrum S Anderson, Anant Kharkar, Bobby Filar, and Phil Roth. Evading machine learning malware detection. *Black Hat*, 2017.
- Battista Biggio, Iginio Corona, Davide Maiorca, Blaine Nelson, Nedim Šrndić, Pavel Laskov, Giorgio Giacinto, and Fabio Roli. Evasion attacks against machine learning at test time. In Hendrik Blockeel, Kristian Kersting, Siegfried Nijssen, and Filip Železný, editors, *Machine Learning and Knowledge Discovery in Databases*, pages 387–402, Berlin, Heidelberg, 2013. Springer Berlin Heidelberg.
- Charles Blundell, Julien Cornebise, Koray Kavukcuoglu, and Daan Wierstra. Weight uncertainty in neural network. In *International Conference on Machine Learning*, pages 1613–1622. PMLR, 2015.
- Jiahao Chen. Fair lending needs explainable models for responsible recommendation. *arXiv preprint arXiv:1809.04684*, 2018.
- Nic Ford, Justin Gilmer, Nicolas Carlini, and Dogus Cubuk. Adversarial examples are a natural consequence of test error in noise. *arXiv preprint arXiv:1901.10513*, 2019.
- Nicholas Frosst, Nicolas Papernot, and Geoffrey Hinton. Analyzing and improving representations with the soft nearest neighbor loss. In Kamalika Chaudhuri and Ruslan Salakhutdinov, editors, *Proceedings of the 36th International Conference on Machine Learning*, volume 97 of *Proceedings of Machine Learning Research*, pages 2012–2020. PMLR, 09–15 Jun 2019. URL <http://proceedings.mlr.press/v97/frosst19a.html>.
- Yarin Gal. Uncertainty in deep learning. *University of Cambridge*, 1(3):4, 2016.
- Yarin Gal and Zoubin Ghahramani. Dropout as a bayesian approximation: Representing model uncertainty in deep learning. In *international conference on machine learning*, pages 1050–1059. PMLR, 2016.
- Yarin Gal, Mark Van Der Wilk, and Carl E Rasmussen. Distributed variational inference in sparse gaussian process regression and latent variable models. *arXiv preprint arXiv:1402.1389*, 2014.
- Zahra Ghodsi, Siva Kumar Sastry Hari, Iuri Frosio, Timothy Tsai, Alejandro Troccoli, Stephen W Keckler, Siddharth Garg, and Anima Anandkumar. Generating and characterizing scenarios for safety testing of autonomous vehicles. *arXiv preprint arXiv:2103.07403*, 2021.
- Shafi Goldwasser, Adam Tauman Kalai, Yael Kalai, and Omar Montasser. Beyond perturbations: Learning guarantees with arbitrary adversarial test examples. In H. Larochelle, M. Ranzato, R. Hadsell, M. F. Balcan, and H. Lin, editors, *Advances in Neural Information Processing Systems*, volume 33, pages 15859–15870. Curran Associates, Inc., 2020. URL <https://proceedings.neurips.cc/paper/2020/file/b6c8cf4c587f2ead0c08955ee6e2502b-Paper.pdf>.
- Ian J Goodfellow, Jonathon Shlens, and Christian Szegedy. Explaining and harnessing adversarial examples. *arXiv preprint arXiv:1412.6572*, 2014.
- Fredrik K Gustafsson, Martin Danelljan, and Thomas B Schon. Evaluating scalable bayesian deep learning methods for robust computer vision. In *Proceedings of the IEEE/CVF Conference on Computer Vision and Pattern Recognition Workshops*, pages 318–319, 2020.
- Dan Hendrycks and Thomas G Dietterich. Benchmarking neural network robustness to common corruptions and surface variations. *arXiv preprint arXiv:1807.01697*, 2018.
- Dan Hendrycks and Kevin Gimpel. A baseline for detecting misclassified and out-of-distribution examples in neural networks. *arXiv preprint arXiv:1610.02136*, 2016.
- Lakshya Jain, Varun Chandrasekaran, Uyeong Jang, Wilson Wu, Andrew Lee, Andy Yan, Steven Chen, Somesh Jha, and Sanjit A Seshia. Analyzing and improving neural networks by generating semantic counterexamples through differentiable rendering. *arXiv preprint arXiv:1910.00727*, 2019.
- Heinrich Jiang, Been Kim, Melody Y Guan, and Maya R Gupta. To trust or not to trust a classifier. In

- NeurIPS*, pages 5546–5557, 2018.
- Daphne Koller and Nir Friedman. *Probabilistic Graphical Models: Principles and Techniques - Adaptive Computation and Machine Learning*. The MIT Press, 2009. ISBN 0262013193.
- Balaji Lakshminarayanan, Alexander Pritzel, and Charles Blundell. Simple and scalable predictive uncertainty estimation using deep ensembles. *arXiv preprint arXiv:1612.01474*, 2016.
- Kimin Lee, Kibok Lee, Honglak Lee, and Jinwoo Shin. A simple unified framework for detecting out-of-distribution samples and adversarial attacks. In S. Bengio, H. Wallach, H. Larochelle, K. Grauman, N. Cesa-Bianchi, and R. Garnett, editors, *Advances in Neural Information Processing Systems*, volume 31. Curran Associates, Inc., 2018. URL <https://proceedings.neurips.cc/paper/2018/file/abdeb6f575ac5c6676b747bca8d09cc2-Paper.pdf>.
- Lydia T Liu, Sarah Dean, Esther Rolf, Max Simchowitz, and Moritz Hardt. Delayed impact of fair machine learning. In *International Conference on Machine Learning*, pages 3150–3158. PMLR, 2018.
- Aleksander Madry, Aleksandar Makelov, Ludwig Schmidt, Dimitris Tsipras, and Adrian Vladu. Towards deep learning models resistant to adversarial attacks. In *International Conference on Learning Representations*, 2018. URL <https://openreview.net/forum?id=rJzIBfZAb>.
- Vaishnavh Nagarajan, Anders Andreassen, and Behnam Neyshabur. Understanding the failure modes of out-of-distribution generalization. In *International Conference on Learning Representations*, 2021. URL [https://openreview.net/forum?id=fSTD6NFIW\\_b](https://openreview.net/forum?id=fSTD6NFIW_b).
- Nicolas Papernot and Patrick D. McDaniel. Deep k-nearest neighbors: Towards confident, interpretable and robust deep learning. *CoRR*, abs/1803.04765, 2018. URL <http://arxiv.org/abs/1803.04765>.
- Jayaram Raghuram, Varun Chandrasekaran, Somesh Jha, and Suman Banerjee. Detecting anomalous inputs to dnn classifiers by joint statistical testing at the layers. *arXiv preprint arXiv:2007.15147*, 2020.
- Carl Edward Rasmussen. Gaussian processes in machine learning. In *Summer school on machine learning*, pages 63–71. Springer, 2003.
- Kevin Roth, Yannic Kilcher, and Thomas Hofmann. The odds are odd: A statistical test for detecting adversarial examples. In Kamalika Chaudhuri and Ruslan Salakhutdinov, editors, *Proceedings of the 36th International Conference on Machine Learning*, volume 97 of *Proceedings of Machine Learning Research*, pages 5498–5507. PMLR, 09–15 Jun 2019. URL <http://proceedings.mlr.press/v97/roth19a.html>.
- Sara Sabour, Yanshuai Cao, Fartash Faghri, and David J. Fleet. Adversarial manipulation of deep representations. In *4th International Conference on Learning Representations, ICLR 2016, San Juan, Puerto Rico, May 2-4, 2016, Conference Track Proceedings*, 2016. URL <http://arxiv.org/abs/1511.05122>.
- C. Scott and R. Nowak. A neyman-pearson approach to statistical learning. 51(11):3806–3819. ISSN 1557-9654. doi: 10.1109/TIT.2005.856955. Conference Name: IEEE Transactions on Information Theory.
- Chawin Sitawarin and David Wagner. On the robustness of deep k-nearest neighbors. In *2019 IEEE Security and Privacy Workshops (SPW)*, pages 1–7. IEEE, 2019.
- Chawin Sitawarin and David Wagner. Minimum-norm adversarial examples on knn and knn based models. In *2020 IEEE Security and Privacy Workshops (SPW)*, pages 34–40. IEEE, 2020.
- Christian Szegedy, Wojciech Zaremba, Ilya Sutskever, Joan Bruna, Dumitru Erhan, Ian Goodfellow, and Rob Fergus. Intriguing properties of neural networks. In *International Conference on Learning Representations*, 2014. URL <http://arxiv.org/abs/1312.6199>.
- Vladimir Vovk and Ruodu Wang. Combining p-values via averaging. 2019. URL <https://arxiv.org/abs/1212.4966>.
- Jingkang Wang, Ava Pun, James Tu, Sivabalan Manivasagam, Abbas Sadat, Sergio Casas, Mengye Ren, and Raquel Urtasun. Advsim: Generating safety-critical scenarios for self-driving vehicles. *arXiv preprint arXiv:2101.06549*, 2021.

## A Additional Information on the Method

### A.1 Pair-wise vs. One-vs-All Distance Testing

For a given layer  $\lambda \in [L]$ , we have the activations per layer for the new test input  $\tilde{\mathbf{X}}_\lambda$  and distances of the nearest neighbors  $\mu_{\lambda,y}$  from each class  $y$ . In the statistical tests, we do *pair-wise* comparison between two classes using the distances  $\mu$  to determine to which class the new input  $\tilde{\mathbf{x}}$  belongs to. The alternative approach is *One-vs-All*, where we test distances from a selected class vs distances from all other classes. We observe that the latter method performs worse. As an illustrative example, if  $\tilde{\mathbf{x}}$  is close to two classes  $A, B$  and very far away from other classes, then these two close classes  $A, B$  are accepted as potential classes for  $\tilde{\mathbf{x}}$ . In such a case, the *pair-wise* comparison between  $A, B$  is required to determine the final class.

We can also construct a case, where the pair-wise comparison is not sufficient. If we consider all the reference (training or calibration) points, then  $\tilde{\mathbf{x}}$  can lie on a a very wide manifold from class  $A$  but can also be surrounded by a circle-like manifold from class  $B$ . If we consider distances of all points from class  $A$  to  $\tilde{\mathbf{x}}$ , then they might be larger than the distances from class  $B$ , even though  $\tilde{\mathbf{x}}$  belongs to class  $A$ . In the multi-dimensional spaces, to alleviate this problem and be able to obtain useful approximation from our distance metric, we have to narrow down the considered space to the vicinity of  $\tilde{\mathbf{x}}$  by finding the  $k$  nearest neighbors.

### A.2 Other Possible Inference Methods Based on $p$ -values

The extreme is to remove a class from consideration if it does not appear in each layer. In other words, if a class does not appear in any neighbor across all layers, we discard the class (as a potential correct prediction). We also have a threshold that there have to be at least 10% neighbors of a given class to consider the class within a layer. If we do not set the significance level, then only 0.4% examples out of 10000 clean MNIST test samples are rejected. Only these samples have confidence lower than 1. All other samples have the confidence of 1 (and their  $p$ -values are equal to 0). On the other hand, only 44% of notmnist samples are rejected and because their confidence is lower than 1 (56%  $p$ -values are equal to 0). Thus, this is a too strict/conservative test. We have to consider more  $p$ -values to obtain higher than 0  $p$ -values and these  $p$ -values should be discriminate enough to distinguish between in distribution and out-of-distribution samples. In the above approach, only 1 out of 1000 samples requires a comparison between 3 classes.

One way to tackle the problem of the too confident predictor is to fill in the missing  $p$ -values. For example, if class  $c1$  is present in all layers while class  $c2$  is only in layers 2,3,4 but absent in layer 1, then we set the  $p$ -value that intuitively denotes the *probability* that class  $c2$  is a better prediction than class  $c1$  in layer 1 to 0. If classes  $c1$  and  $c2$  are considered in some layers but both are absent from, e.g., the first layer, then we set the corresponding  $p$ -values to 1 for both classes in this first layer. This allows us to set the threshold of 5% acceptance rate for in distribution samples using a significance level of 0.05, however, the acceptance rate of the out-of-distribution samples is about 33% (the previous method gave only about 19%).

The *occam* method (with dictionary of dictionaries) can converge to the the *combine* method (a combination of  $p$ -values in tensors). We have to fill in the missing values using  $p$ -value 0 or 1. This has to be done, for instance, on the level of layers, where some classes are missing in some layers, and on the level of the class aggregation when there are missing classes from consideration (they do not appear in the nearest neighbors found). The *occam* method has a more complex implementation so we retain the *combine* method as our primary one.

## B Details for Experiments from Table 3

Note, we do not strictly follow the weighted average from Vovk and Wang (2019) but weight the  $p$ -values before the (standard) averaging and then multiply by the factor  $\min(2, \frac{1}{\max(w)})$ , where  $w$  is the vector of weights per layer. We do a few simplifications compared to Algorithm 1 and present the steps in Algorithm 3.

For results in Table 3, we present the classification accuracy for the datasets and methods in Table 4 and the parameters used in Tables 5 and 6.

We follow the setup from Papernot and McDaniel (2018) and use the same deep network architecture (as described there in Table III) as well as the parameters for FGSM and PGD (BIM) attacks (Table II).

---

**Algorithm 3**  $p$ -DkNN prediction algorithm for results from Table 3.

---

**Input:** Test point:  $\tilde{\mathbf{x}}$ , test point activations:  $\{\tilde{\mathbf{x}}_\lambda\}_{\lambda=1}^L$ , activations from the training set:  $\{\mathbf{X}_\lambda\}_{\lambda=1}^L$ , labels from the training set:  $\mathbf{y}$ , number of neighbors:  $k$ , significance level:  $\alpha$ .

**Output:** Classification  $\tilde{y} \in [C]$  or abstain  $\perp$

```

45 for  $\lambda \in [L]$  do
46    $\mu \leftarrow \text{get\_distances}(\mathbf{X}_\lambda, \tilde{\mathbf{x}}_\lambda)$ 
47    $\hat{\mu}, \text{indices} \leftarrow \text{get\_smallest}(\mu, k)$ 
48    $\hat{\mathbf{y}} \leftarrow \text{get\_classes}(\mathbf{y}, \text{indices})$ 
49    $\mathcal{P}_\lambda \leftarrow \text{pairwise\_t}(\mu, \hat{\mathbf{y}})$ 
50 end
51  $\mathbf{p} \leftarrow \text{aggregate\_p}(\mathcal{P})$ 
52  $\tilde{p} \leftarrow \min(\mathbf{p})$ 
53  $\tilde{y} \leftarrow \text{argmin}(\mathbf{p})$ 
54 if  $\tilde{p} < \alpha$  then
55   return  $\tilde{y}$ 
56 end
57 return  $\perp$ 

```

---

Table 4: **Classification accuracy** of the models from Table 3 on the entire test set.

| MODEL     | MNIST | FASHIONMNIST | SVHN | GTSRB |
|-----------|-------|--------------|------|-------|
| NN        | .988  | .905         | .902 | .928  |
| DkNN      | .988  | .897         | .904 | .930  |
| $p$ -DkNN | .991  | .907         | .901 | .914  |

Table 5: **Parameters** for the classifiers from Table 3 for MNIST and FashionMNIST.  $\tau$  is the confidence threshold,  $k$  is number of nearest neighbors,  $w$  are weights per layer.

| MODEL     | MNIST  |     |                 | FASHIONMNIST |     |             |
|-----------|--------|-----|-----------------|--------------|-----|-------------|
|           | $\tau$ | $k$ | $w$             | $\tau$       | $k$ | $w$         |
| NN        | .974   | N/A | N/A             | .952         | N/A | N/A         |
| DkNN      | .05    | 75  | N/A             | .11          | 75  | N/A         |
| $p$ -DkNN | .0019  | 100 | .02 .02 .02 .94 | .025         | 100 | .1 .1 .1 .7 |

Table 6: **Parameters** for the classifiers from Table 3 for SVHN and GTSRB.  $\tau$  is the confidence threshold,  $k$  is number of nearest neighbors,  $w$  are weights per layer.

| MODEL     | SVHN   |     |                 | GTSRB  |     |                  |
|-----------|--------|-----|-----------------|--------|-----|------------------|
|           | $\tau$ | $k$ | $w$             | $\tau$ | $k$ | $w$              |
| NN        | .672   | N/A | N/A             | .870   | N/A | N/A              |
| DkNN      | .08    | 75  | N/A             | .04    | 75  | N/A              |
| $p$ -DkNN | .15    | 100 | .05 .07 .07 .81 | .058   | 100 | .05 .05 .1 .1 .7 |

Table 7: **Average confidence**  $\mu$  for the classifiers from Table 3.

| ATTACK      | MODEL     | MNIST | FASHIONMNIST | SVHN | GTSRB |
|-------------|-----------|-------|--------------|------|-------|
| NONE        | NN        | .99   | .977         | .921 | .958  |
|             | DkNN      | .663  | .552         | .451 | .460  |
|             | $p$ -DkNN | .991  | .969         | .953 | .955  |
| OOD1        | NN        | .942  | .952         | .688 | .549  |
|             | DkNN      | .063  | .142         | .088 | .066  |
|             | $p$ -DkNN | .937  | .941         | .783 | .821  |
| OOD2        | NN        | .607  | .977         | .700 | .597  |
|             | DkNN      | .046  | .552         | .017 | .073  |
|             | $p$ -DkNN | .943  | .969         | .787 | .820  |
| FEAT        | NN        | .0    | .850         | .788 | .677  |
|             | DkNN      | .071  | .191         | .170 | .117  |
|             | $p$ -DkNN | .754  | .944         | .849 | .865  |
| FGSM        | NN        | .929  | .984         | .867 | .765  |
|             | DkNN      | .073  | .205         | .125 | .131  |
|             | $p$ -DkNN | .956  | .942         | .826 | .861  |
| PGD         | NN        | .999  | 1.0          | 1.0  | 1.0   |
|             | DkNN      | .141  | .219         | .378 | .352  |
|             | $p$ -DkNN | .975  | .948         | .957 | .943  |
| $\angle 45$ | NN        | .837  | .914         | .693 | .813  |
|             | DkNN      | .166  | .093         | .061 | .156  |
|             | $p$ -DkNN | .972  | .933         | .764 | .877  |

## C Potential Negative Societal Impacts of Our Work

Our work aims at improving the inference of the already trained neural network classifiers. Thus, we focus on a general-purpose methodology and not specific applications that could have more direct potential impact on society. On the other hand, we can imagine that our method could be used to train a classifier that refrains from providing answers for specific ethnic groups and classifying them as OOD. To mitigate such a harm, the train and validation sets should include samples for all possible ethnic groups.